JCI insight

Fibroblast-specific deletion of interleukin-1 receptor-1 reduces adverse cardiac remodeling following myocardial infarction

Sumia A. Bageghni, Karen E. Hemmings, Nadira Y. Yuldasheva, Azhar Maqbool, Filomena O. Gamboa-Esteves, Neil E. Humphreys, Maj Simonsen Jackson, Christopher P. Denton, Sheila Francis, Karen E. Porter, Justin F. X. Ainscough, Emmanuel Pinteaux, Mark J. Drinkhill, Neil A. Turner

JCI Insight. 2019. https://doi.org/10.1172/jci.insight.125074.

Research In-Press Preview **Cardiology** **Inflammation**

It has been hypothesized that interleukin-1alpha (IL-1α) is released from damaged cardiomyocytes following myocardial infarction (MI) and activates cardiac fibroblasts via its receptor (IL-1R1) to drive the early stages of cardiac remodeling. This study aimed to definitively test this hypothesis using cell type-specific IL-1α and IL-1R1 knockout (KO) mouse models. A floxed *Il1α* mouse was created and used to generate a cardiomyocyte-specific IL-1α KO mouse line (MIL1AKO). A tamoxifen-inducible fibroblast-specific IL-1R1 hemizygous KO mouse line (FIL1R1KO) was also generated. Mice underwent experimental MI (permanent left anterior descending coronary artery ligation) and cardiac function was determined 4 weeks later by conductance pressure-volume catheter analysis. Molecular markers of remodeling were evaluated at various time points by real-time RT-PCR and histology. MIL1AKO mice showed no difference in cardiac function or molecular markers of remodeling post-MI compared with littermate controls. In contrast, FIL1R1KO mice showed improved cardiac function and reduced remodeling markers post-MI compared with littermate controls. In conclusion, these data highlight a key role for the IL-1R1/cardiac fibroblast signaling axis in regulating post-MI remodeling and provide support for the continued development of anti-IL-1 therapies for improving cardiac function after MI. Cardiomyocyte-derived IL-1α was not an important contributor to post-MI remodeling in this model.

Fibroblast-specific Deletion of Interleukin-1 Receptor-1 Reduces Adverse Cardiac Remodeling Following Myocardial Infarction

Sumia A. Bageghni,[1=] Karen E. Hemmings,[1=] Nadira Y. Yuldasheva,[1] Azhar Maqbool,[1] Filomena O. Gamboa-Esteves,[2] Neil E. Humphreys,[3] Maj Simonsen Jackson,[3] Christopher P. Denton,[4] Sheila Francis,[5] Karen E. Porter,[1] Justin F. X. Ainscough,[1] Emmanuel Pinteaux,[3] Mark J. Drinkhill,[1=] and Neil A. Turner[1]

[1] Discovery and Translational Science Department, Leeds Institute of Cardiovascular and Metabolic Medicine (LICAMM), School of Medicine, University of Leeds, Leeds, LS2 9JT, UK. [2] Leeds Institute of Cancer and Pathology, Leeds Teaching Hospitals NHS Trust, Leeds LS9 7TF, UK. [3] Faculty of Biology, Medicine and Health, AV Hill Building, University of Manchester, Oxford Road, Manchester M13 9PT, UK. [4] Institute of Immunity and Transplantation, Centre for Rheumatology and Connective Tissue Diseases, University College London and Royal Free Hospital, Rowland Hill Street, London NW3 2PF, UK. [5] Department of Infection, Immunity & Cardiovascular Disease, Medical School, University of Sheffield, Sheffield S10 2RX, UK.

[=] These authors (SAB, KEH and MJD) contributed equally to this work.

NEH's present address: EMBL-Rome, Epigenetics and Neurobiology Unit, Via Ramarini 32, 00015 Monterotondo (RM), Italy.
JFXA's present address: Department of Biology, University of York, Heslington, York, YO10 5DD, UK.

Address for correspondence: Dr Neil A. Turner, Discovery and Translational Science Department, Leeds Institute of Cardiovascular and Metabolic Medicine (LICAMM), LIGHT Laboratories, Clarendon Way, University of Leeds, Leeds LS2 9JT, UK. Tel: +44(0)113-3434817. E-mail: n.a.turner@leeds.ac.uk

Conflict of interest: The authors have declared that no conflict of interest exists

The funding agency requires a Creative Commons CC-BY license in order to support publication fees for this manuscript.

Abstract

It has been hypothesized that interleukin-1α (IL-1α) is released from damaged cardiomyocytes following myocardial infarction (MI) and activates cardiac fibroblasts via its receptor (IL-1R1) to drive the early stages of cardiac remodeling. This study aimed to definitively test this hypothesis using cell type-specific IL-1α and IL-1R1 knockout (KO) mouse models. A floxed *Il1a* mouse was created and used to generate a cardiomyocyte-specific IL-1α KO mouse line (MIL1AKO). A tamoxifen-inducible fibroblast-specific IL-1R1 hemizygous KO mouse line (FIL1R1KO) was also generated. Mice underwent experimental MI (permanent left anterior descending coronary artery ligation) and cardiac function was determined 4 weeks later by conductance pressure-volume catheter analysis. Molecular markers of remodeling were evaluated at various time points by real-time RT-PCR and histology. MIL1AKO mice showed no difference in cardiac function or molecular markers of remodeling post-MI compared with littermate controls. In contrast, FIL1R1KO mice showed improved cardiac function and reduced remodeling markers post-MI compared with littermate controls. In conclusion, these data highlight a key role for the IL-1R1/cardiac fibroblast signaling axis in regulating post-MI remodeling and provide support for the continued development of anti-IL-1 therapies for improving cardiac function after MI. Cardiomyocyte-derived IL-1α was not an important contributor to post-MI remodeling in this model.

Introduction

Although widely recognized as key regulators of extracellular matrix (ECM) turnover, cardiac fibroblasts also have wide-reaching functions that are fundamental to the overall physiology and pathophysiology of the heart, including sensing tissue damage and contributing to cardiac inflammation (1,2). Cardiac fibroblasts are particularly responsive to the proinflammatory cytokine interleukin (IL)-1 (3), whose levels are increased with many cardiovascular pathologies including myocardial infarction (MI), cardiomyopathy, myocarditis and hypertension (4,5). In response to IL-1 stimulation, cardiac fibroblasts secrete an array of proinflammatory cytokines and chemokines, and enhance ECM turnover through increased secretion of matrix metalloproteinases (MMPs), decreased collagen synthesis and decreased expression of profibrotic cytokines (3). Thus, fibroblasts can contribute to the inflammatory milieu that occurs in the myocardium early after MI, and the IL-1/cardiac fibroblast signaling axis is a potentially important mediator of post-MI cardiac remodeling (2,3). Furthermore, there is growing evidence to suggest that IL-1 blockade is a viable therapeutic strategy for treating cardiovascular disease (6-8).

IL-1 comprises two distinct gene products (IL-1α and IL-1β) that have generally indistinguishable biological activities and play a significant role in the pathogenesis of heart disease (4). Despite their similarity of action, IL-1α and IL-1β are produced by cells through very different mechanisms. IL-1α is an intracellular cytokine (nuclear and cytosolic) that is released when cells undergo necrosis and was originally shown to be a key trigger for inflammation in the liver (9). Importantly, it has also been proposed that IL-1α release from necrotic cardiomyocytes acts in a similar manner, triggering the early inflammatory response after MI (10). This key role for IL-1α in post-MI inflammation has been supported by a recent murine study in which an IL-1α-specific blocking antibody reduced myocardial injury and improved cardiac function after experimental MI (11). In contrast to IL-1α, IL-1β is inactive until it undergoes inflammasome-mediated proteolytic processing prior to non-classical secretion from cells in response to specific stimuli (12). In mice, cardiomyocytes express both IL-1α and IL-1β, whereas cardiac fibroblasts express IL-1β, but not IL-1α (10).

Irrespective of their differences in expression, synthesis, activation and secretion, the biological effects of both IL-1α and IL-1β are mediated through the same receptor, interleukin-1 receptor-1 (IL-1R1). Ligand binding to IL-1R1 stimulates its association with the IL-1 receptor accessory protein (IL-1RacP) which in turn recruits the MyD88 and IRAK4 signaling proteins to form a stable tetrameric signaling module in which all components are

essential (13). The downstream functional effects of IL-1 are mediated primarily via MAP kinase (ERK, p38, JNK) and NF-κB signaling pathways which are stimulated following recruitment of further adaptor proteins and kinases to the core IL-1R1 signaling module (3,13).

Studies on IL-1R1 global knockout (KO) mice have revealed a critical role for IL-1R1 in mediating cardiac myofibroblast accumulation, MMP expression and fibrotic remodeling of the infarcted heart (14-16). The beneficial effects observed in IL-1R1 KO mice were largely the result of suppressed inflammation, however direct effects on cardiac fibroblasts were also suggested (14). Nevertheless, the global nature of these IL-1R1 KO models makes it difficult to evaluate the precise contribution of IL-1 signaling in cardiac fibroblasts.

Taken together, these in vivo and in vitro studies suggest that interplay between IL-1α (released from damaged cardiomyocytes) and IL-1R1 activation (on cardiac fibroblasts) is critical in the early myocardial remodeling process after MI. However, to date no studies have sought to directly evaluate the importance of these interactions in vivo in a cell-specific context. The aim of this study was to use cell type-specific KO mouse models to investigate the role of cardiomyocyte IL-1α and fibroblast IL-1R1 in regulating post-MI cardiac remodeling.

Results

Cardiomyocyte-specific IL-1α knockout does not affect cardiac function or remodeling after experimental MI

A cardiomyocyte-specific IL-1α KO mouse model was generated to evaluate the contribution of cardiomyocyte-derived IL-1α to cardiac remodeling after MI. Firstly, a floxed *Il1a* mouse was created in which exon 4 of the *Il1a* gene was modified to be flanked by loxP sites (**Figure 1A, Supplemental Figure 1A**). Floxed *Il1a* mice were then bred with mice expressing Cre recombinase under control of the cardiomyocyte-specific *Myh6* promoter to produce Cre-positive cardiac myocyte-specific IL-1α KO (MIL1AKO) mice and control Cre-negative floxed littermates (**Supplemental Figure 1B**). Deletion PCR confirmed that Cre-positive MIL1AKO mice had the expected deletion within exon 4 of the *Il1a* gene, and that this was only apparent in heart tissue (**Figure 1B**). Mean *Il1a* mRNA expression levels in whole heart samples from control mice were relatively low and were further reduced in hearts from MIL1AKO mice (**Figure 1D**), reflecting *Il1a* gene deletion in the cardiomyocyte

population of the heart. Baseline cardiac characteristics in control (Cre-negative *Il1a*$^{fl/fl}$) and MIL1AKO (Cre-positive *Il1a*$^{fl/fl}$) mice were assessed by pressure-volume (P-V) conductance catheter analysis and showed no difference between groups (**Supplemental Figure 2A**). Basal expression levels of remodeling genes (collagens and hypertrophy markers) were also similar for the two lines (**Supplemental Figure 2B**). Thus, Cre-induced deletion of IL-1α in cardiomyocytes had no effect on the baseline cardiac phenotype of the animals.

To determine the impact of cardiomyocyte-specific IL-1α KO on post-MI function and remodeling, we used a permanent left anterior descending (LAD) coronary artery ligation model of experimental MI. Male Cre-negative (control) and Cre-positive (MIL1AKO) littermates underwent LAD ligation at 10-12 weeks of age (**Figure 1C**) and cardiac physiological measurements were obtained 4 weeks later by P-V conductance catheter analysis (**Figure 1E**). MI scarring was clearly visible in hearts obtained from animals that had undergone LAD ligation (**Figure 2A**).

As expected, control mice displayed overt cardiac dysfunction 4 weeks after MI, as evidenced by reduced ejection fraction (EF), increased end systolic volume (ESV) and increased end diastolic volume (EDV) compared to sham animals (**Figure 1E**), with other parameters being unaffected (**Supplemental Table 1**). Importantly, no difference in post-MI cardiac function was observed between control mice and MIL1AKO mice (**Figure 1E**, **Supplemental Table 1**), indicating that cardiomyocyte-derived IL-1α *per se* was not an important contributor to cardiac dysfunction after MI.

Assessment of gene expression in the infarct region 3 days after MI by real-time quantitative reverse transcription PCR (qRT-PCR) revealed increases in mRNA levels of inflammatory genes (*Il1b*, *Tnfa*, *Il6*) and ECM regulatory genes (*Mmp3*, *Mmp9, Tnc, Postn, Col1a1, Col3a1*), and reduced mRNA for the myofibroblast differentiation marker *Acta2* in MI hearts compared to sham hearts (**Figure 1F**). Importantly, there was no difference in expression levels of these genes between control and MIL1AKO mice after MI (**Figure 1F**). Histological analysis of hearts 4 weeks after MI revealed no obvious differences between control and MIL1AKO mice, with both showing thinning of the LV free wall in the infarct area and scar tissue marked by ECM deposition (**Figure 2B**), in agreement with the functional and mRNA expression data.

Characterization of fibroblast-specific IL-1R1 knockout mouse model

Having ruled out a role for cardiomyocyte-derived IL-1α in modulating cardiac remodeling after MI, we proceeded to investigate the specific role of the IL-1 receptor (IL-1R1) expressed by cardiac fibroblasts. *Col1a2*-CreER(T) mice have previously been used to induce Cre-lox-mediated deletion of genes specifically in fibroblasts (17), including those in the heart (18-20), without affecting cardiomyocytes, endothelial cells, smooth muscle cells, progenitor cells, pericytes or macrophages. We firstly developed a *Col1a2*-Cre-*Il1r1*$^{fl/fl}$ mouse line (see **Supplemental Figure 3A** for breeding strategy) to explore the effects of fibroblast-specific IL1R1 deletion on cardiac remodeling. However, this method was ineffective at reducing IL1R1 expression or activation in cardiac fibroblasts (data not shown), despite our previous success with this approach for deleting other genes (20). To overcome this problem we adopted a modified strategy to generate a hemizygous mouse line with global deletion of one *Il1r1* allele in which the remaining allele was floxed. This approach is particularly useful for targeting genes whose heterozygous (+/-) KO does not cause a phenotype as it maximizes the impact of inducible KO of the remaining allele (21).

Therefore we first generated global IL-1R1$^{+/-}$ heterozygous mice and IL-1R1$^{-/-}$ KO mice (see **Supplemental Figure 3B** for breeding strategy) to investigate the phenotypic effect of mono-allelic and bi-allelic deletion of *Il1r1*. As expected, primary cultures of cardiac fibroblasts from heterozygous animals exhibited a 50% reduction in *Il1r1* mRNA levels compared with wild type mice, with no detectable expression in those from IL-1R1 KO mice (**Figure 3A**). The functional impact of fibroblast IL1R1 KO was evaluated in cultured cardiac fibroblasts by measuring IL-1α responses; specifically kinase signaling pathways, gene expression and protein secretion. IL-1α stimulated the p38 and NF-κB signaling pathways (**Figure 3B**) and increased *Il6*, *Mmp3* and *Mmp9* mRNA expression (**Figure 3C**) and IL-6 and MMP-3 protein secretion (**Figure 3D**) to a similar extent in fibroblasts from wild-type and heterozygous mice, despite the latter expressing only half the amount of IL-1R1. Cardiac fibroblasts from IL-1R1 KO mice did not respond to IL-1α stimulation (**Figure 3B-D**), confirming full loss of the receptor. Responses to TNFα, a proinflammatory cytokine that activates similar signaling pathways and gene expression profiles to IL-1α but via a different receptor, were unaffected in cardiac fibroblasts from IL-1R1 KO mice (**Figure 3B,E**). Together, these data establish that full biallelic deletion of *Il1r1* is necessary to disrupt IL-1 responses in cardiac fibroblasts and that mono-allelic deletion is ineffective.

We next generated hemizygous mice in which one *Il1r1* allele was floxed and the other was deleted (fl/-). These animals were crossed with heterozygous mice that expressed

tamoxifen-inducible Cre recombinase (CreER(T)) under the control of the fibroblast-specific *Col1a2* promoter (**Figure 4A**) to generate *Col1a2*-CreER(T)-*Il1r1*$^{fl/-}$ mice; a line we named FIL1R1KO (see **Supplemental Figure 3C** for breeding strategy). Example genotyping results are shown in **Supplemental Figure 4**. Mice were injected with tamoxifen at 12 days of age to induce Cre-loxP-mediated deletion, and hearts isolated after a further 4-8 weeks for analysis. The efficiency of fibroblast-specific deletion of IL-1R1 was confirmed in primary cultures of cardiac fibroblasts by qRT-PCR. Cells from FIL1R1KO mice had a mean 75% reduction in basal *Il1r1* mRNA levels compared with cells from Cre-negative *Il1r1*$^{fl/-}$ littermate control mice (**Figure 4B**), indicating that full biallelic deletion of *Il1r1* had occurred in response to tamoxifen in ~75% of cardiac fibroblasts. The functional impact of IL-1R1 deletion was evidenced by a marked reduction in the activation of the p38 and NF-κB signaling pathways in response to IL-1α, without affecting TNFα-induced signaling (**Figure 4C**). Moreover, mean IL-1α-induced *Il6*, *Mmp3* and *Mmp9* mRNA expression was reduced by 65-75% in fibroblasts cultured from FIL1R1KO hearts compared with cells from control littermate hearts (**Figure 4D**); in close agreement with the extent of IL1R1 knockdown (**Figure 4B**). Similar changes were noted for protein secretion; for example mean IL-1α-induced IL-6 secretion was reduced by >50% in cardiac fibroblasts from FIL1R1KO mice (**Figure 4E**).

Fibroblast-specific IL-1R1 knockout improves cardiac remodeling after experimental MI

Having confirmed functional and sustained knockdown of IL-1R1 in cardiac fibroblasts isolated from tamoxifen-treated FIL1R1KO mice, we next investigated the in vivo impact of fibroblast-selective IL-1R1 deletion on cardiac function after experimental MI (**Figure 5A**). Male Cre-negative (control) and Cre-positive (FIL1R1KO) littermates were injected with tamoxifen at 12 days of age for 5 consecutive days and underwent permanent LAD coronary artery ligation surgery at 10-12 weeks of age. Sham control animals (pooled Cre-negative and Cre-positive) were not injected with tamoxifen. There were no differences in baseline cardiac characteristics between Cre-positive and Cre-negative mice (**Supplemental Figure 5**). Physiological measurements were obtained 4 weeks after LAD ligation by P-V catheter analysis, before hearts were analyzed for histological and molecular markers of remodeling. P-V analysis (**Figure 5B, Supplemental Table 2**) revealed significantly reduced EF in control mice 4 weeks after MI compared with sham (48% versus 61% respectively; P=0.02), but importantly EF was only partially reduced to 56% in FIL1R1KO mice after MI and was

not significantly different to sham controls. dPdtmax (an indicator of contractility) was also significantly decreased in control MI mice compared with sham, but was less affected in FIL1R1KO mice, and not significantly different from sham animals. Similar, non-significant trends were observed with ESV and EDV (**Figure 5B, Supplemental Table 2**). End systolic pressures were significantly reduced in MI mice of both genotypes compared with sham animals whereas other cardiac parameters and arterial blood pressure were not significantly different between the three groups (**Supplemental Table 2**).

The impact of fibroblast-selective IL-1R1 deletion on specific molecular markers of cardiac remodeling was assessed by qRT-PCR of whole ventricle mRNA samples taken from hearts used for P-V analysis (i.e. 4 weeks after LAD ligation). Nine genes were studied that included markers of ECM synthesis (*Col1a1*, *Col3a1*), ECM degradation (*Mmp3*, *Mmp9*), myofibroblast activation (*Acta2*), mechanical activation (*Tnc, Il6*) and cardiomyocyte hypertrophy (*Myh7*, *Nppa*). Significant increases in *Col1a1* (1.7-fold increase; $P<0.05$), *Col3a1* (3.2-fold; $P<0.001$), *Mmp3* (2.5-fold; $P<0.05$) and *Tnc* (2.1-fold; $P<0.05$) mRNA levels were observed in control post-MI hearts compared with sham hearts (**Figure 5C**). By comparison, the expression levels of all four of these genes was markedly less in post-MI hearts from FIL1R1KO mice [*Col1a1* (1.3-fold increase), *Col3a1* (1.8-fold; $P<0.05$ versus control MI), *Mmp3* (1.7-fold), *Tnc* (1.3-fold)] and, with the exception of *Col3a1*, were not significantly different from sham levels (**Figure 5C**).

Histological staining was performed on hearts 5 days (**Figure 6**) or 6 weeks (**Figure 7**) after MI. In control mice, granulation tissue was evidenced after 5 days by inflammatory cell infiltration (**Figure 6,** H&E) and marked tenascin C expression (**Figure 6**), with a small amount of collagen expression (**Figure 6,** MVG). After 6 weeks, control mice had evidence of ventricular wall thinning (**Figure 7**) and more collagen deposition (**Figure 7,** MVG), with very little tenascin C expression (**Figure 7**). All these changes were more pronounced in control mice compared with FIL1R1KO mice (**Figure 6 & 7**).

Discussion

We used two novel cell-specific KO mouse models to investigate the role of cardiomyocyte-derived IL-1α and the cardiac fibroblast IL-1 receptor, IL-1R1, in remodeling of the heart post-MI. The principal conclusion of our study was that fibroblast-specific deletion of IL-1R1 was cardioprotective following MI, whereas cardiomyocyte-specific deletion of IL-1α had no effect. Our data with FIL1R1KO mice suggest that fibroblast IL-1R1 signaling is a significant

driver of detrimental cardiac remodeling post-MI. In vitro studies have revealed that cardiac fibroblasts adopt a pro-inflammatory, pro-angiogenic, pro-migratory, ECM-degrading, non-differentiated phenotype in response to IL-1 [3]. Our in vivo observations suggest that these acute effects of IL-1 on cardiac fibroblasts early after MI contribute to longer-term adverse cardiac remodeling that is detrimental to cardiac function. These data support ongoing strategies aimed at inhibiting IL-1 or its receptor to improve cardiac function post-MI (6-8).

Role of IL-1α

Cardiomyocyte-specific overexpression of human IL-1α induces cardiac hypertrophy in mice (22). Moreover, it has been proposed by Lugrin and colleagues that cardiomyocyte-derived IL-1α is important for stimulating the early inflammatory response post-MI (10). On the contrary, we observed no difference in cardiac function or expression of remodeling genes post-MI in a cardiomyocyte-specific IL-1α KO mouse (MIL1AKO) compared with control mice, suggesting that cardiomyocyte-derived IL-1α is not an essential player in this process. It is worth noting several differences between our study and that of Lugrin et al (10). Firstly, we used a cardiomyocyte-specific IL-1α KO mouse, whereas their study used global IL-1α KO mice, so it is possible that the effects that were observed therein were due to IL-1α deletion in non-myocyte cells (e.g. endothelial cells, fibroblasts, inflammatory cells), which together account for 70% of cells in the murine heart (23). Secondly, the experimental MI model used in that other study (10) was an ischemia-reperfusion model of MI as opposed to the permanent LAD ligation model we used. Although the ischemia-reperfusion model more closely resembles the clinical scenario where most patients undergo revascularization, the permanent occlusion model is particularly useful for understanding direct mechanisms without the confounding element of reperfusion. We chose the permanent occlusion model based on previous studies showing that interference of IL-1 signaling had favorable effects in both non-reperfusion (16) and reperfusion models (10,14). Finally, Lugrin et al (10), did not evaluate longer-term functional endpoints, with all measurements being taken immediately after the reperfusion period (2 hours). One of the markers studied was IL-6, whose increase was reduced in global IL-1α KO mice after the 2 h reperfusion period (10). In contrast, in our study, *Il6* mRNA levels remained significantly elevated 3 days after permanent LAD occlusion and were not affected by cardiomyocyte-specific IL-1α deletion, indicating there was no long-term impact on inflammation.

Our results do not preclude an important role for IL-1α *per se*, and indeed there is recent evidence that cardiac IL-1α is important in post-MI cardiac remodeling, as administration of an IL-1α neutralizing antibody reduced infarct size and preserved LV systolic function in an ischemia-reperfusion model of MI (11). Although we observed that basal cardiac *Il1a* mRNA levels were very low, and were further reduced in MIL1AKO mice, IL-1α release can still occur in our model from non-myocyte cells, including endothelial cells, fibroblasts and macrophages; all of which may contribute to cardiac IL-1α levels after MI.

Role of IL-1β

Although our study did not directly investigate the contribution of IL-1β to post-MI remodeling, our data with the FIL1R1KO mouse may indicate a role for IL-1β acting on fibroblast IL-1R1. Indeed, such a role is supported by mouse and rat studies in which anti-IL-1β neutralizing antibodies administered after MI improve cardiac function and limit adverse remodeling (24,25). IL-1β is produced by multiple cardiac cell types (26) and can directly promote adverse cardiac remodeling (4).

Clinical relevance

Therapeutic IL-1 blockade has now been evaluated in several cardiovascular clinical trials (reviewed in (6-8)). Initially, a number of small-scale trials investigated the effect of Anakinra, a recombinant form of the IL-1 receptor antagonist, on inflammation and cardiac remodeling in stable-STEMI and non-STEMI patients (27,28), reporting that IL-1 inhibition reduced post-MI inflammation, but had little effect on cardiac function in the longer term. This may relate to the relatively mild inflammatory phenotype in these patient cohorts compared with general STEMI patients, in whom IL-1 blockade was more effective (29). A more recent Anakinra trial (D-HART2) reported that IL-1 blockade did not improve cardiorespiratory fitness in obese HF patients with preserved ejection fraction, although markers of systemic inflammation and myocardial strain were reduced (30). In comparison to general IL-1 blockade with Anakinra, the recent CANTOS trial used an IL-1β-specific neutralizing antibody (Canakinumab) and reported a reduction in cardiovascular events independent of lipid levels (31), with a suggestion that the cardioprotective effects extended beyond new atherothrombotic events. Thus, there is gathering momentum for the use of

targeted anti-IL-1 therapies for improving outcome after MI, at least in some patient populations.

Study limitations

Although our study provided evidence for a role of fibroblast IL-1R1 in driving adverse cardiac remodeling, it remains unclear whether IL-1α or IL-1β (or both) is the most important stimulus. Our results with MIL1AKO mice ruled out a role for cardiomyocyte-derived IL-1α, but other cellular sources of IL-1α were not explored. Future studies investigating selective IL-1α KO in other cardiac cell types (fibroblasts, endothelial cells, macrophages) will be required to explore this further. Similarly, global or cell-specific IL-1β KO mice would be helpful in determining the precise role of IL-1β in this setting. We used a permanent LAD ligation model of MI; investigations with an ischemia-reperfusion model of MI would be important to confirm our data in a more clinically appropriate model. We did not evaluate the area at risk in our MI models; although this might have been useful to understand the underlying mechanisms for cardioprotection in FIL1R1KO mice. Although we studied specific features of remodeling by quantifying expression levels of specific genes, and provided representative histological images, a more in-depth quantitative analysis of inflammation and fibrosis using supportive methodologies (e.g. flow cytometry and hydroxyproline incorporation respectively) would have strengthened our conclusions. Prolonged cardiomyocyte-specific Cre expression has been reported to result in modest cardiac dysfunction, fibrosis and hypertrophy in 6 month old *Myh6*-Cre mice (32), but not in 3 month old mice (32,33). The MIL1AKO mice used in the current study were 10-12 weeks of age at the time of surgery and, although not directly addressed in our study, it is therefore unlikely that age-dependent Cre cardiotoxicity influenced the data.

Conclusion

Our data highlight the importance of the IL-1/cardiac fibroblast signaling axis in regulating post-MI remodeling and provide support for the continued development of anti-IL-1 therapies for improving cardiac function post-MI.

Methods

Animal welfare

Mice were maintained in individually ventilated cages at 21°C, 50-70% humidity, 12/12 h light/dark cycle with Pure-o'Cel paper bedding (Datesand) and *ad libitum* access to water and RM1 diet (Special Diets Services).

Mouse models

Floxed mice: Floxed *Il1a* (exon 4) mice were created as follows. *Il1a*$^{tm1a(EUCOMM)Wtsi}$ embryonic stem cells (34) were purchased from the European Mouse Mutant Cell Repository (EuMMCR). Cells from clone EPD0822-4-H02 were prepared for microinjection according to the previously published protocol (35) with minor modifications. Briefly, cells were cultured in KO-DMEM + KOSR medium + 2i (MEK inhibitor and GSK3 inhibitor) on a gelatin-coated (0.1% gelatin in phosphate buffered saline) cell culture dish maintained under standard culture conditions (37°C, 5% CO_2, humidified). Culture medium was changed daily and cells were passaged when 75-80% confluent using accutase to dissociate them. Cells were passaged no more than 3 times, and were transferred to media without 2i reagents for 24 h prior to microinjection. Cells were then microinjected into 4 to 8 cell B6N-Tyr^{c-Brd}/BrdCrCrl embryos. Surviving embryos were surgically implanted into the oviduct of day 0.5 post-coitum pseudopregnant mice. Resulting black/white C57BL/6N chimeras were back-crossed onto C57BL/6N wild-type mice to assess germline penetrance. Potential founder mice were screened by PCR for LacZ, Neo and LoxP sites. This line was further crossed with C57BL/6N-Tg(CAG-Flpo)1Afst/Mmucd mice from the Mutant Mouse Resource & Research Centers (MMRRC). The FLP recombinase expression provided by this line resulted in a "conditional ready" (i.e. floxed) *Il1a*$^{tm1c(EUCOMM)Wtsi}$ allele in which exon 4 is flanked by loxP sites. Floxed *Il1r1* (exon 5) mice have been described previously (36) and were provided by Emmanuel Pinteaux (University of Manchester, UK).

Cre-expressing mice: Cardiomyocyte-specific *Myh6*-Cre mice (011038) and PGK-Cre global deleter mice (020811) were obtained from The Jackson Laboratory (www.jax.org). Fibroblast-specific tamoxifen-inducible *Col1a2*-Cre-ER(T) mice have been well characterized (17,37) and were provided by Christopher Denton (University College London, UK).

Breeding of cardiomyocyte-specific and fibroblast-specific KO mice: The breeding strategy to obtain cardiomyocyte-specific IL-1α KO mice (**Supplemental Figure 1B**) involved crossing

homozygous *Il1a*$^{fl/fl}$ mice with heterozygous *Myh6*-Cre mice to generate *Myh6*-Cre-*Il1a*$^{fl/fl}$ mice. When these were back-crossed with *Il1a*$^{fl/fl}$ mice, Cre-positive cardiac myocyte-specific IL-1α KO mice ("MIL1AKO") and Cre-negative floxed littermates (control) were produced.

For investigating IL-1R1 in cardiac fibroblasts, a tamoxifen-inducible fibroblast-specific IL-1R1 KO mouse line (*Col1a2*-CreER(T)-*Il1r1*$^{fl/fl}$) was initially established on a C57BL/6 background by crossing *Col1a2*-CreER(T) mice with *Il1r1*$^{fl/fl}$ mice (**Supplemental Figure 3A**). Global IL-1R1 KO mice were subsequently established by crossing female PGK-Cre mice with male *Il1r1*$^{fl/fl}$ mice on a C57BL/6 background (**Supplemental Figure 3B**). Finally, a tamoxifen-inducible fibroblast-specific IL-1R1 hemizygous KO mouse line "FIL1R1KO" (*Col1a2*-CreER(T)-*Il1r1*$^{fl/-}$) was established by crossing heterozygous *Col1a2*-Cre-ER(T) mice with *Il1r1*$^{fl/fl}$ mice on a C57BL/6 background (**Supplemental Figure 3C**).

Tamoxifen-inducible Cre activation

For the fibroblast-targeted studies, control (Cre-negative *Il1r1*$^{fl/-}$) and FIL1R1KO mice were injected with tamoxifen dissolved in corn oil (100 mg/kg/day i.p. for 5 consecutive days) at 12 days of age to induce CreER(T) activity and facilitate Cre/loxP-mediated deletion in Cre-positive fibroblasts.

Genotyping PCR

For routine genotyping, DNA was extracted from lysed ear notch / tissue samples using tail lysis buffer supplemented with proteinase K as described (20), and end-point PCR performed with specific primer pairs (**Supplemental Table 3**) before resolving by agarose gel electrophoresis. Routine genotyping was subsequently outsourced to Transnetyx (Cordova, TN, USA) for automated analysis.

End-point PCR was also used to confirm cardiomyocyte-specific deletion of *Il1a* exon 4 in whole heart tissue and fibroblast-specific deletion of *Il1r1* exon 5 in cultured cardiac fibroblasts using specific primer sets (**Supplemental Table 3**).

Experimental MI model

A permanent LAD coronary artery ligation model of experimental MI was performed on 5% isoflurane-anaesthetized male mice (10-12 weeks of age), as we described previously (38). Following intubation, mice were ventilated at a tidal volume of 140 μl and a respiratory rate of 120/min with 1.5% isoflurane and 100% oxygen. The LAD was ligated at the edge of the

left atrium using 8-0 prolene suture and occlusion confirmed by observing pallor of the anterior LV wall.

For cardiomyocyte-targeted mice, LAD ligation was performed on Cre-positive (MIL1AKO) and Cre-negative (control) littermates. For fibroblast-targeted mice, LAD ligation was performed on Cre-positive (FIL1R1KO) and Cre-negative (control) littermates that had been injected with tamoxifen at 12 days of age. Sham operated animals (no tamoxifen treatment) underwent a similar surgical procedure without tying the ligature. In order to keep the number of animals used to a minimum, sham data was combined from the two different genotypes (Cre-positive and Cre-negative), which showed no differences in baseline phenotype.

Measurement of cardiac function

Physiological measurements of cardiac function were obtained by Millar conductance P-V catheter analysis, as we have described in full previously (20,39). The investigator performing the P-V measurements was blinded to the genotype of the animals.

Histology

Hearts were extracted at various time points and fixed in 4% paraformaldehyde before paraffin wax-embedding. Tissue sections (5 μm) were stained as we described previously with Miller's elastic van Gieson (MVG) stain (40) or with antibodies for tenascin-C (Santa Cruz Biotechnology sc-8694) (38). Composite tiled images were prepared from individual photomicrographs so that cross-sections through the whole heart could be observed.

Real-time qRT-PCR

RNA was purified from cells or snap-frozen heart tissue, and cDNA synthesis performed as described previously (20). Real-time qRT-PCR was undertaken using an ABI-7500 System with specific Taqman primer/probe sets (Applied Biosystems) for detecting *Acta2* (Mm00725412_s1), *Col1a1* (Mm00801666_g1), *Col3a1* (Mm01254476_m1), *Gapdh* (Mm99999915_g1), *Il1a* (Mm99999060_m1), *Il1b* (Mm00434228_m1), *Il1r1* (Mm01226961), *Il6* (Mm00446190_m1), *Mmp3* (Mm00440295_m1), *Mmp9* (Mm00442991_m1), *Myh7* (Mm00600555_m1), *Nppa* (Mm01255747_g1), *Postn* (Mm01284919_m1), *Tnc* (Mm00495662_m1) and *Tnfa* (Mm00443258_m1). Data are expressed relative to *Gapdh* mRNA expression using the $2^{-\Delta CT}$ method.

Cardiac fibroblast culture

Cardiac fibroblasts were cultured from mouse hearts by a collagenase digestion method, as we described previously (20,41). Experiments were performed in serum-free medium using early passage (P0 or P1) cells.

Immunoblotting

Immunoblotting was performed as described previously (42) using Cell Signaling Technology antibodies for phospho-p38 (#9211) and IκB-α expression (#9242). β-actin expression (loading control) was detected with Abcam ab8226 antibody. Horseradish peroxidase-conjugated secondary antibodies and enhanced chemiluminescence detection reagent were from GE Healthcare. Blots were imaged using G:BOX gel doc system (Syngene) and band intensities quantified using GeneTools software (Syngene).

Statistics

Statistical analyses were conducted using GraphPad Prism 7.01 Software (www.graphpad.com). Unless stated otherwise, data are mean values ± SEM. Box plots illustrate median, 25^{th}/75^{th} percentiles and minimum/maximum. The n value represents the number of separate animals or the number of cell cultures from separate hearts (i.e. biological replicates). Data were analyzed by 2-tailed t-test, 2-way ANOVA (with Bonferroni post hoc) or 1-way ANOVA (with Tukey post hoc), as appropriate. A P value less than 0.05 was considered significant.

Study approval

All animal procedures were carried out in accordance with the Animal Scientific Procedures Act (UK) 1986 under UK Home Office authorization following review by the University of Leeds Animal Welfare and Ethical Review Committee.

Author contributions

SAB, KEH, MJD and NAT designed the experiments. SAB, KEH, MJD, AM, NYY, FOG-E, NEH and MS-J conducted the experiments. SAB, KEH, MJD and NAT analyzed the data. CPD and EP provided reagents or tools. NAT, MJD, EP, SF, JFXA and KEP obtained

funding for this work. NAT conceptualized the study and wrote the manuscript. All authors commented on and approved the submission of this work.

Acknowledgments

We are grateful to the British Heart Foundation, UK who funded this research through project grants PG/11/80/29135 (NAT, MJD, JFXA and KEP), PG/16/31/32130 (NAT, MJD and EP) and PG/13/55/30365 (SF and EP). We also gratefully acknowledge Dr Elena Redondo-Castro and Dr Matthew Baxter (University of Manchester, UK) for culturing embryonic stem cells.

References

1. Chen W and Frangogiannis NG. Fibroblasts in post-infarction inflammation and cardiac repair. *Biochim Biophys Acta* 2013;1833:945-953.

2. Turner NA. Inflammatory and fibrotic responses of cardiac fibroblasts to myocardial damage associated molecular patterns (DAMPs). *J Mol Cell Cardiol* 2016;94:189-200.

3. Turner NA. Effects of interleukin-1 on cardiac fibroblast function: Relevance to post-myocardial infarction remodelling. *Vascul Pharmacol* 2014;60:1-7.

4. Frangogiannis NG. Interleukin-1 in cardiac injury, repair, and remodeling: pathophysiologic and translational concepts. *Discoveries (Craiova)* 2015;3.

5. Guillen I, Blanes M, Gomez-Lechon MJ, Castell JV. Cytokine signaling during myocardial infarction: sequential appearance of IL-1 beta and IL-6. *Am J Physiol* 1995;269:R229-R235.

6. Buckley LF and Abbate A. Interleukin-1 blockade in cardiovascular diseases: a clinical update. *Eur Heart J* 2018;39:2063-2069.

7. Huang S and Frangogiannis NG. Anti-inflammatory therapies in myocardial infarction: failures, hopes and challenges. *Br J Pharmacol* 2018;175:1377-1400.

8. Libby P. Interleukin-1 beta as a target for atherosclerosis therapy: biological basis of CANTOS and beyond. *J Am Coll Cardiol* 2017;70:2278-2289.

9. Chen CJ, Kono H, Golenbock D, Reed G, Akira S, Rock KL. Identification of a key pathway required for the sterile inflammatory response triggered by dying cells. *Nat Med* 2007;13:851-856.

10. Lugrin J, Parapanov R, Rosenblatt-Velin N, Rignault-Clerc S, Feihl F, Waeber B, Muller O, Vergely C, Zeller M, Tardivel A *et al*. Cutting Edge: IL-1α is a crucial danger signal triggering acute myocardial inflammation during myocardial infarction. *J Immunol* 2015;194:499-503.

11. Mauro AG, Mezzaroma E, Torrado J, Kundur P, Joshi P, Stroud K, Quaini F, Lagrasta CA, Abbate A, Toldo S. Reduction of myocardial ischemia-reperfusion injury by inhibiting interleukin-1 alpha. *J Cardiovasc Pharmacol* 2017;69:156-160.

12. Martin-Sanchez F, Diamond C, Zeitler M, Gomez AI, Baroja-Mazo A, Bagnall J, Spiller D, White M, Daniels MJ, Mortellaro A *et al*. Inflammasome-dependent IL-1β release depends upon membrane permeabilisation. *Cell Death Differ* 2016;23:1219-1231.

13. Weber A, Wasiliew P, Kracht M. Interleukin-1 (IL-1) pathway. *Sci Signal* 2010;3:cm1.

14. Bujak M, Dobaczewski M, Chatila K, Mendoza LH, Li N, Reddy A, Frangogiannis NG. Interleukin-1 receptor type I signaling critically regulates infarct healing and cardiac remodeling. *Am J Pathol* 2008;173:57-67.

15. Saxena A, Chen W, Su Y, Rai V, Uche OU, Li N, Frangogiannis NG. IL-1 induces proinflammatory leukocyte infiltration and regulates fibroblast phenotype in the infarcted myocardium. *J Immunol* 2013;191:4838-4848.

16. Abbate A, Salloum FN, Van Tassell BW, Vecile E, Toldo S, Seropian I, Mezzaroma E, Dobrina A. Alterations in the interleukin-1/interleukin-1 receptor antagonist balance modulate cardiac remodeling following myocardial infarction in the mouse. *PLoS One* 2011;6:e27923.

17. Denton CP, Khan K, Hoyles RK, Shiwen X, Leoni P, Chen Y, Eastwood M, Abraham DJ. Inducible lineage-specific deletion of TβRII in fibroblasts defines a pivotal regulatory role during adult skin wound healing. *J Invest Dermatol* 2009;129:194-204.

18. Lal H, Ahmad F, Zhou J, Yu JE, Vagnozzi RJ, Guo Y, Yu D, Tsai EJ, Woodgett J, Gao E *et al*. Cardiac fibroblast glycogen synthase kinase-3β regulates ventricular remodeling and dysfunction in ischemic heart. *Circulation* 2014;130:419-430.

19. Ubil E, Duan J, Pillai IC, Rosa-Garrido M, Wu Y, Bargiacchi F, Lu Y, Stanbouly S, Huang J, Rojas M *et al*. Mesenchymal-endothelial transition contributes to cardiac neovascularization. *Nature* 2014;514:585-590.

20. Bageghni SA, Hemmings KE, Zava N, Denton CP, Porter KE, Ainscough JFX, Drinkhill MJ, Turner NA. Cardiac fibroblast-specific p38α MAP kinase promotes cardiac hypertrophy via a putative paracrine interleukin-6 signaling mechanism. *FASEB J* 2018;32:4941-4954.

21. Feil,S., Valtcheva,N., and Feil,R. 2009. Inducible Cre mice. In Gene Knockout Protocols. R.Kuhn and Wurst,W., editors. Humana Press, 343-362.

22. Nishikawa K, Yoshida M, Kusuhara M, Ishigami N, Isoda K, Miyazaki K, Ohsuzu F. Left ventricular hypertrophy in mice with a cardiac-specific overexpression of interleukin-1. *Am J Physiol Heart Circ Physiol* 2006;291:H176-H183.

23. Pinto AR, Ilinykh A, Ivey MJ, Kuwabara JT, D'Antoni ML, Debuque R, Chandran A, Wang L, Arora K, Rosenthal NA *et al*. Revisiting cardiac cellular composition. *Circ Res* 2016;118:400-409.

24. Toldo S, Mezzaroma E, Van Tassell BW, Farkas D, Marchetti C, Voelkel NF, Abbate A. Interleukin-1β blockade improves cardiac remodelling after myocardial infarction without interrupting the inflammasome in the mouse. *Exp Physiol* 2013;98:734-745.

25. Harouki N, Nicol L, Remy-Jouet I, Henry JP, Dumesnil A, Lejeune A, Renet S, Golding F, Djerada Z, Wecker D *et al*. The IL-1β antibody gevokizumab limits cardiac remodeling and coronary dysfunction in rats with heart failure. *JACC Basic Transl Sci* 2017;2:418-430.

26. Christia P, Bujak M, Gonzalez-Quesada C, Chen W, Dobaczewski M, Reddy A, Frangogiannis NG. Systematic characterization of myocardial inflammation, repair, and remodeling in a mouse model of reperfused myocardial infarction. *J Histochem Cytochem* 2013;61:555-570.

27. Abbate A, Van Tassell BW, Biondi-Zoccai G, Kontos MC, Grizzard JD, Spillman DW, Oddi C, Roberts CS, Melchior RD, Mueller GH *et al*. Effects of interleukin-1 blockade with Anakinra on adverse cardiac remodeling and heart failure after acute myocardial infarction [from the Virginia Commonwealth University-Anakinra Remodeling Trial 2 (VCU-ART2) Pilot Study]. *Am J Cardiol* 2013;111:1394-1400.

28. Morton AC, Rothman AM, Greenwood JP, Gunn J, Chase A, Clarke B, Hall AS, Fox K, Foley C, Banya W *et al*. The effect of interleukin-1 receptor antagonist therapy on markers of inflammation in non-ST elevation acute coronary syndromes: the MRC-ILA Heart Study. *Eur Heart J* 2015;36:377-384.

29. Abbate A, Kontos MC, Grizzard JD, Biondi-Zoccai GG, Van Tassell BW, Robati R, Roach LM, Arena RA, Roberts CS, Varma A *et al*. Interleukin-1 blockade with anakinra to prevent adverse cardiac remodeling after acute myocardial infarction (Virginia Commonwealth University Anakinra Remodeling Trial [VCU-ART] Pilot study). *Am J Cardiol* 2010;105:1371-1377.

30. Van Tassell BW, Trankle CR, Canada JM, Carbone S, Buckley L, Kadariya D, Del Buono MG, Billingsley H, Wohlford G, Viscusi M *et al*. IL-1 blockade in patients with heart failure with preserved ejection fraction. *Circ Heart Fail* 2018;11:e005036.

31. Ridker PM, Everett BM, Thuren T, MacFadyen JG, Chang WH, Ballantyne C, Fonseca F, Nicolau J, Koenig W, Anker SD *et al*. Antiinflammatory therapy with canakinumab for atherosclerotic disease. *N Engl J Med* 2017;377:1119-1131.

32. Pugach EK, Richmond PA, Azofeifa JG, Dowell RD, Leinwand LA. Prolonged Cre expression driven by the alpha-myosin heavy chain promoter can be cardiotoxic. *J Mol Cell Cardiol* 2015;86:54-61.

33. Fan D, Takawale A, Shen M, Samokhvalov V, Basu R, Patel V, Wang X, Fernandez-Patron C, Seubert JM, Oudit GY *et al*. A disintegrin and metalloprotease-17 regulates pressure overload-induced myocardial hypertrophy and dysfunction through proteolytic processing of integrin β1. *Hypertension* 2016;68:937-948.

34. Skarnes WC, Rosen B, West AP, Koutsourakis M, Bushell W, Iyer V, Mujica AO, Thomas M, Harrow J, Cox T *et al*. A conditional knockout resource for the genome-wide study of mouse gene function. *Nature* 2011;474:337-342.

35. Gertsenstein M, Nutter LM, Reid T, Pereira M, Stanford WL, Rossant J, Nagy A. Efficient generation of germ line transmitting chimeras from C57BL/6N ES cells by aggregation with outbred host embryos. *PLoS One* 2010;5:e11260.

36. Abdulaal WH, Walker CR, Costello R, Redondo-Castro E, Mufazalov IA, Papaemmanouil A, Rothwell NJ, Allan SM, Waisman A, Pinteaux E *et al*. Characterization of a conditional interleukin-1 receptor 1 mouse mutant using the Cre/LoxP system. *Eur J Immunol* 2016;46:912-918.

37. Zheng B, Zhang Z, Black CM, de Crombrugghe B, Denton CP. Ligand-dependent genetic recombination in fibroblasts : a potentially powerful technique for investigating gene function in fibrosis. *Am J Pathol* 2002;160:1609-1617.

38. Maqbool A, Spary EJ, Manfield IW, Ruhmann M, Zuliani-Alvarez L, Gamboa-Esteves FO, Porter KE, Drinkhill MJ, Midwood KS, Turner NA. Tenascin C upregulates interleukin-6 expression in human cardiac myofibroblasts via toll-like receptor 4. *World J Cardiol* 2016;8:340-350.

39. Frentzou GA, Drinkhill MJ, Turner NA, Ball SG, Ainscough JF. A state of reversible compensated ventricular dysfunction precedes pathological remodelling in response to cardiomyocyte-specific activity of angiotensin II type-1 receptor in mice. *Dis Model Mech* 2015;8:783-794.

40. Yuldasheva NY, Rashid ST, Haywood NJ, Cordell P, Mughal R, Viswambharan H, Imrie H, Sukumar P, Cubbon RM, Aziz A *et al*. Haploinsufficiency of the insulin-like growth factor-1 receptor enhances endothelial repair and favorably modifies angiogenic progenitor cell phenotype. *Arterioscler Thromb Vasc Biol* 2014;34:2051-2058.

41. Mylonas KJ, Turner NA, Bageghni SA, Kenyon CJ, White CI, McGregor K, Kimmitt RA, Sulston R, Kelly V, Walker BR *et al*. 11β-HSD1 suppresses cardiac fibroblast CXCL2, CXCL5 and neutrophil recruitment to the heart post MI. *J Endocrinol* 2017;233:315-327.

42. Turner NA, Ball SG, Balmforth AJ. The mechanism of angiotensin II-induced extracellular signal-regulated kinase-1/2 activation is independent of angiotensin AT_{1A} receptor internalisation. *Cell Signal* 2001;13:269-277.

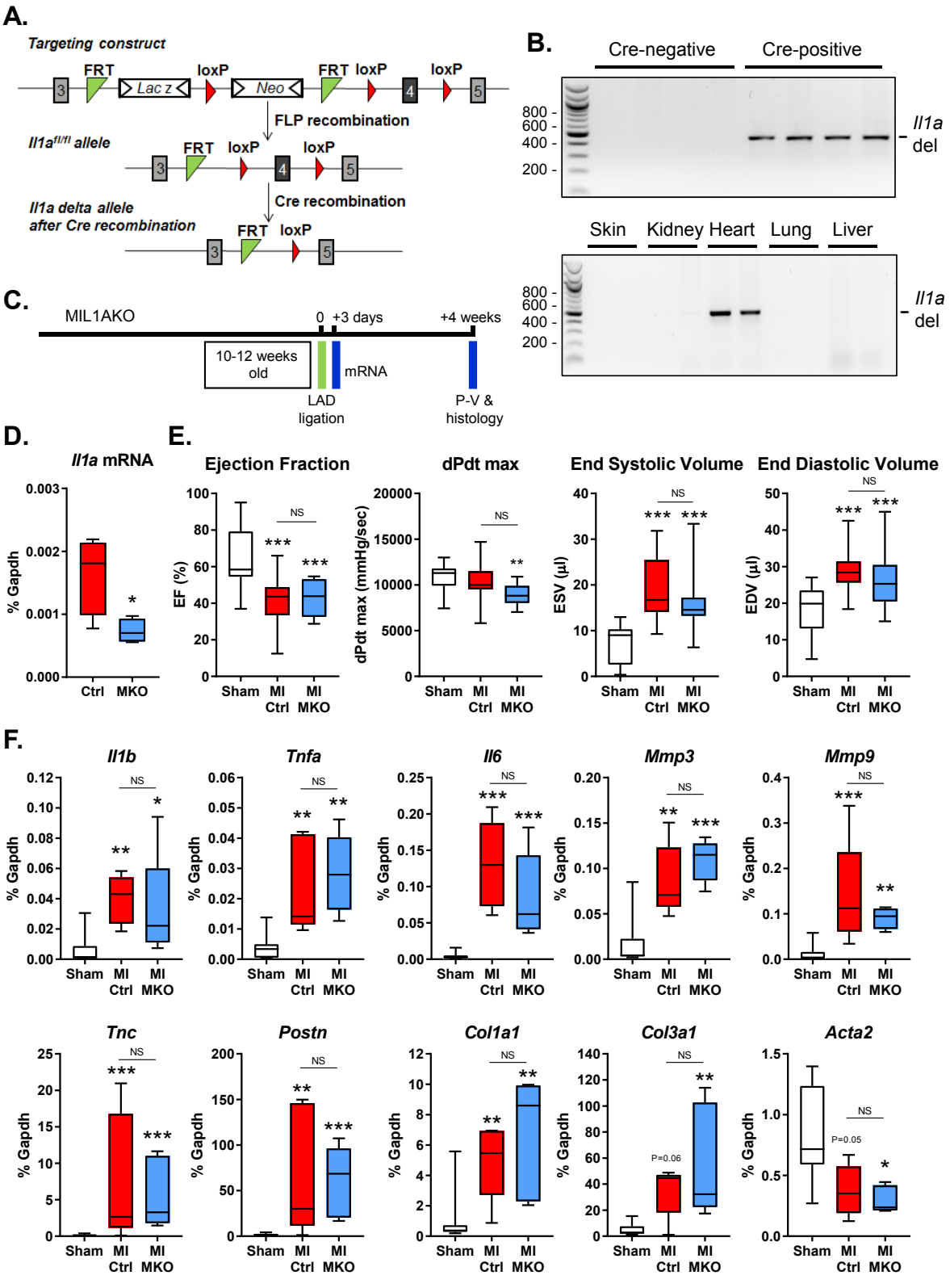

Figure 1. Creation, characterization and functional assessment of cardiomyocyte-specific IL-1α knockout mouse line (MIL1AKO). (A) Generation of floxed interleukin-1α (exon 4) mice: *Il1a*$^{fl/fl}$. Genetic targeting shows exon 4 flanked by loxP sites, positioned

upstream of a lacZ/Neo resistance cassette, which is excised upon Flp recombination, resulting in the generation of *Il1a*$^{fl/fl}$ allele. Cre recombinase leads to exon 4 deletion, generating IL-1α knockout (KO) mice. **(B)** Genotyping showing exon 4 deletion of *Il1a* gene. Size markers (bp) are to the left. *Upper panel:* PCR analysis for *Il1a* exon 4 deletion (456 bp) in cardiac tissue from Cre-negative *Il1a*$^{fl/fl}$ and *Myh6*-Cre-positive *Il1a*$^{fl/fl}$ (MIL1AKO) mice. *Lower panel:* PCR analysis for exon 4 deletion (456 bp) in various tissues in Cre-positive MIL1AKO mice, confirming cardiac-specific deletion. See Supplemental Table 3 for primer details. **(C)** Timeline showing experimental myocardial infarction (MI) induced by ligation of the left anterior descending (LAD) coronary artery and time points for collection of RNA, histology and measurement of cardiac function by pressure-volume (P-V) conductance catheter. **(D)** qRT-PCR analysis of basal *Il1a* mRNA expression in hearts from control (Ctrl; Cre-negative *Il1a*$^{fl/fl}$) and MIL1AKO (MKO; *Myh6*-Cre-positive *Il1a*$^{fl/fl}$) mice. *P<0.05 for effect of KO (unpaired t-test, n=4). **(E)** P-V conductance catheter data. Sham = mixed genotypes (n=19); MI Ctrl = Cre-negative *Il1a*$^{fl/fl}$ after MI (n=19); MI MKO = *Myh6*-Cre-positive *Il1a*$^{fl/fl}$ (MIL1AKO) after MI (n=17). ***P<0.05 versus sham; NS = not significant between the 2 MI groups (1-way ANOVA with Tukey post hoc). **(F)** qRT-PCR data showing relative mRNA levels of remodeling genes interleukin-1β (*Il1b*), tumor necrosis factor α (*Tnfa*), interleukin-6 (*Il6*), matrix metalloproteinases 3 and 9 (*Mmp3*, *Mmp9*), tenascin C (*Tnc*), α-smooth muscle actin (*Acta2*), periostin (*Postn*), collagen Iα1 (*Col1a1*) and collagen IIIα1 (*Col3a1*). Sham = mixed genotypes (n=7); MI Ctrl = Cre-negative *Il1a*$^{fl/fl}$ after MI (n=5); MI MKO = *Myh6*-Cre-positive *Il1a*$^{fl/fl}$ (MIL1AKO) after MI (n=5). ***P<0.01, **P<0.01, *P<0.05 versus sham; NS = not significant between MI groups (1-way ANOVA with Tukey post hoc).

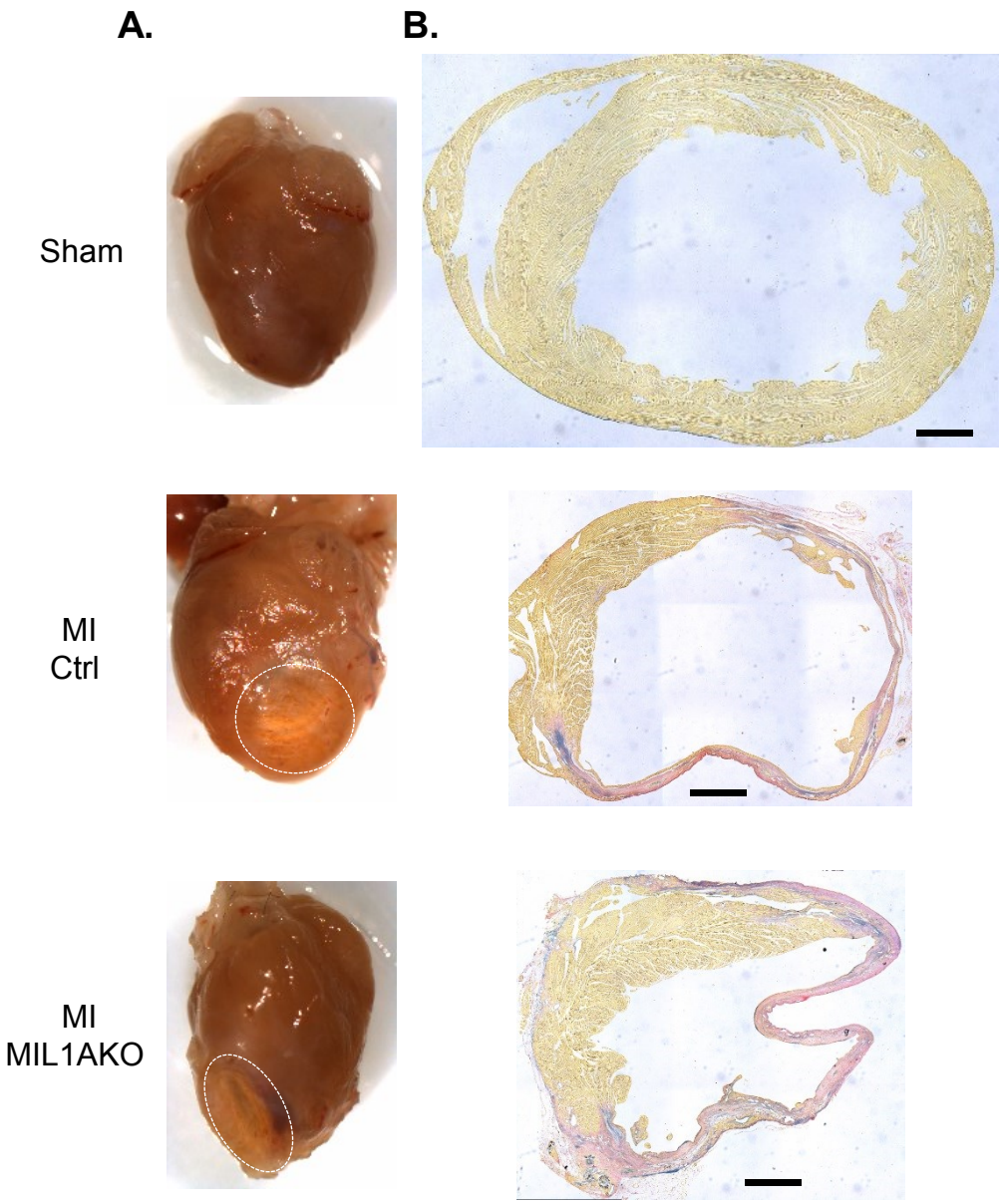

Figure 2. Effect of cardiomyocyte-specific IL-1α deletion on cardiac remodeling post-MI. (A) Representative photographs of sham and myocardial infarction (MI) hearts at end of experimental period (4 weeks after surgery). Sham = mixed genotypes; MI Ctrl = Cre-negative *Il1a*$^{fl/fl}$ after MI; MI MIL1AKO = *Myh6*-Cre-positive *Il1a*$^{fl/fl}$ after MI (n=5). Dashed line = infarcted area. **(B)** Representative photomicrographs of histological sections of hearts stained with Miller's elastic van Gieson. Yellow stain = muscle, pink = collagen, purple = elastin. Scale bars: 700 μm.

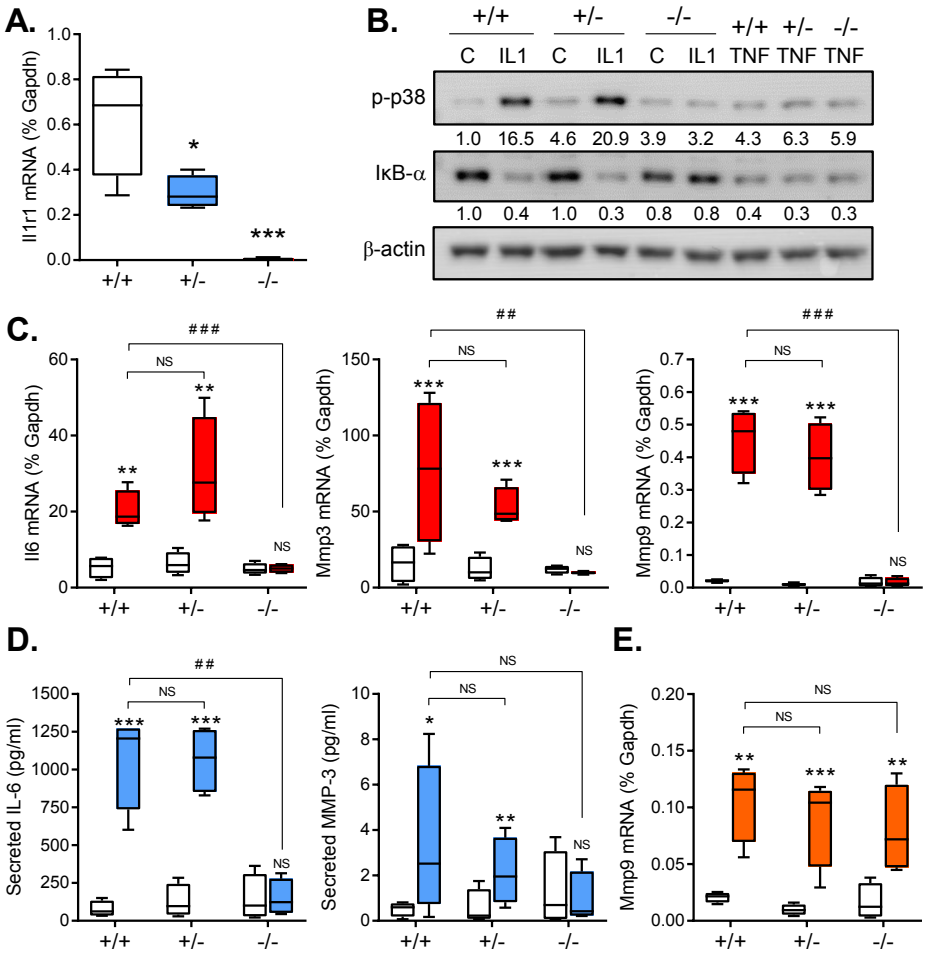

Figure 3. Effect of global IL-1R1 knockout on cardiac fibroblast responses to inflammatory cytokines. (A) qRT-PCR data showing basal interleukin-1 receptor 1 (*Il1r1*) mRNA levels in cardiac fibroblasts cultured from wild-type (+/+), IL-1R1 heterozygote (+/-) and IL-1R1 knockout (KO) (-/-) mice (all n=4). ***P<0.01, *P<0.05 versus wild-type (1-way ANOVA with Tukey post hoc). **(B)** Cardiac fibroblasts were exposed to vehicle control ('C'), 1 ng/ml interleukin-1α (IL1) or 10 ng/ml tumor necrosis factor α (TNF) for 30 min. Immunoblotting was used to measure activation of p38 MAP kinase (phosphorylation; p-p38) or activation of IκB-α (proteasome-mediated degradation). β-actin = loading control. Numbers under blots represent densitometric analysis relative to β-actin and normalized to lane 1. Representative of 2 separate experiments. **(C,D)** Cardiac fibroblasts were treated with vehicle (open boxes) or 1 ng/ml IL-1α (closed boxes) for 6 h before measuring mRNA levels of interleukin-6 (*Il6*) and matrix metalloproteinases 3 and 9 (*Mmp3*, *Mmp9*) by qRT-PCR (*C*) and protein secretion by ELISA (*D*). **(E)** Cardiac fibroblasts were treated with vehicle (open boxes) or 10 ng/ml TNFα (closed boxes) for 6 h before measuring *Mmp9* mRNA levels by qRT-PCR. ***P<0.01, **P<0.01, *P<0.05, NS = not significant for effect of cytokine. $^{###}$P<0.01, $^{##}$P<0.01, NS = not significant for effect of IL-1R1 KO (2-way ANOVA with Bonferroni post hoc). n=4 per genotype.

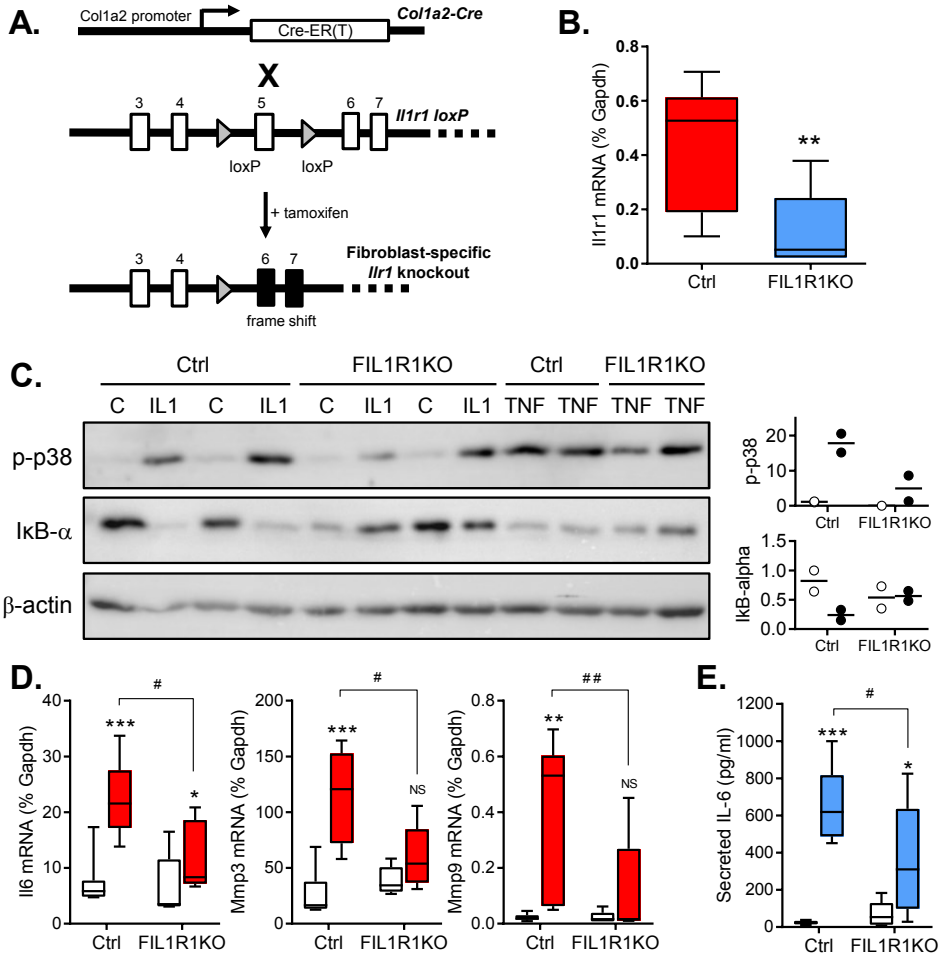

Figure 4. Effect of tamoxifen-induced fibroblast-specific IL-1R1 knockdown on cardiac fibroblast responses to IL-1. (A) Schematic showing loxP-targeted Cre-mediated deletion of exon 5 within the interleukin-1 receptor-1gene, *Il1r1*. **(B-E)** Fibroblast cultures were established from hearts of Cre-negative (Ctrl; n=7) and Cre-positive (fibroblast-specific interleukin-1 receptor 1 knockout [FIL1R1KO]; n=5) hemizygous $Il1r1^{fl/-}$ mice 6 weeks after tamoxifen injection. (*B*) qRT-PCR analysis of basal *Il1r1* mRNA expression in cardiac fibroblasts from Ctrl and FIL1R1KO mice. **P<0.01 for effect of KO (unpaired t-test). *(C)* Cardiac fibroblasts with different genotypes were exposed to vehicle (control, C), interleukin-1α (IL-1) or tumor necrosis factor α (TNF) for 30 min before immunoblotting to measure activation of p38 MAP kinase (phosphorylation; p-p38) or activation of IκB-α (proteasome-mediated degradation). β-actin = loading control. Plots to the right depict densitometric analysis relative to β-actin and normalized to lane 1 for control (open symbols) or IL-1 treatment (closed symbols). n=2. *(D,E)* Cardiac fibroblasts were treated with vehicle (open boxes) or 1 ng/ml IL-1α (closed boxes) for 6 h before measuring mRNA levels of interleukin-6 (*Il6*) and matrix metalloproteinases 3 and 9 (*Mmp3*, *Mmp9*) by qRT-PCR (*D*), and IL-6 secretion by ELISA (*E*). ***P<0.001, **P<0.01, *P<0.05, NS = not significant for effect of IL-1; $^{\#\#}$P<0.01, $^{\#}$P<0.05 for effect of IL-1R1 KO (2-way ANOVA with Bonferroni post hoc).

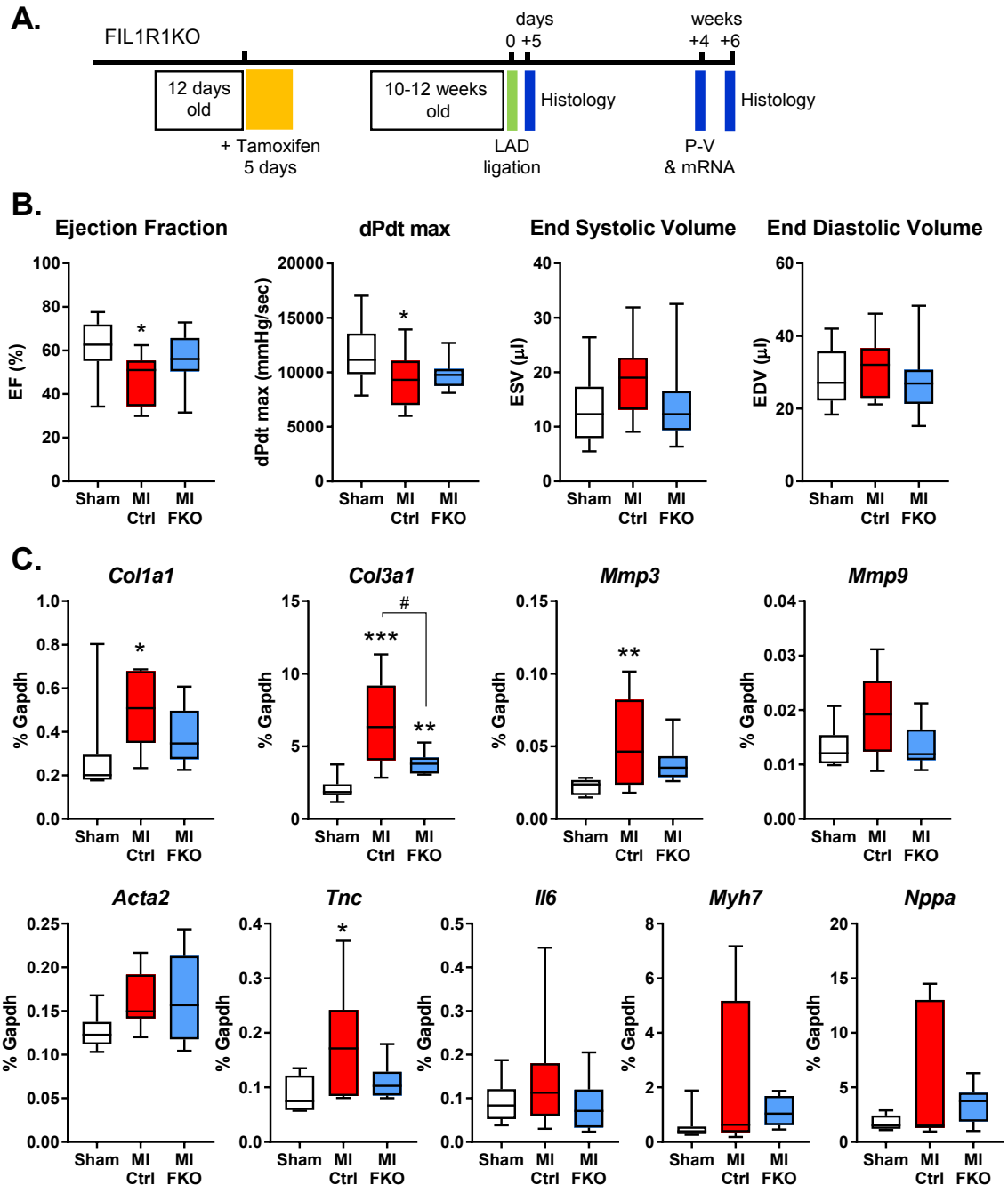

Figure 5. Effect of fibroblast-specific IL-1R1 deletion on cardiac function and remodeling genes 4 weeks post-MI. (A) Experimental timeline showing timing of tamoxifen injection and experimental myocardial infarction (MI) induced by ligation of the left anterior descending (LAD) coronary artery, as well as timings for histology, collection of RNA, and measurement of cardiac function by pressure-volume (P-V) conductance catheter. **(B)** P-V conductance catheter data. Sham = mixed genotypes, no tamoxifen treatment (n=18); MI Ctrl = tamoxifen-treated Cre-negative *Il1r1*$^{fl/-}$ after MI (n=11); MI FKO = tamoxifen-treated Cre-positive *Il1r1*$^{fl/-}$ (FIL1R1KO; fibroblast-specific interleukin-1 receptor 1 knockout) after MI

(n=11). *P<0.05 versus sham. **(C)** qRT-PCR data showing relative mRNA levels of remodeling genes collagen Iα1 (*Col1a1*), collagen IIIα1 (*Col3a1*), matrix metalloproteinases 3 and 9 (*Mmp3*, *Mmp9*), α-smooth muscle actin (*Acta2*), tenascin C (*Tnc*), interleukin-6 (*Il6*), β-myosin heavy chain (*Myh7*) and atrial natriuretic factor (*Nppa*). Sham = mixed genotypes, no tamoxifen treatment (n=8); MI Ctrl = tamoxifen-treated Cre-negative mice after MI (n=8); MI FKO = tamoxifen-treated FIL1R1KO mice after MI (n=8). ***P<0.01, **P<0.01, *P<0.05 versus sham; $^{\#}$P<0.05 versus MI Ctrl (1-way ANOVA with Tukey post hoc).

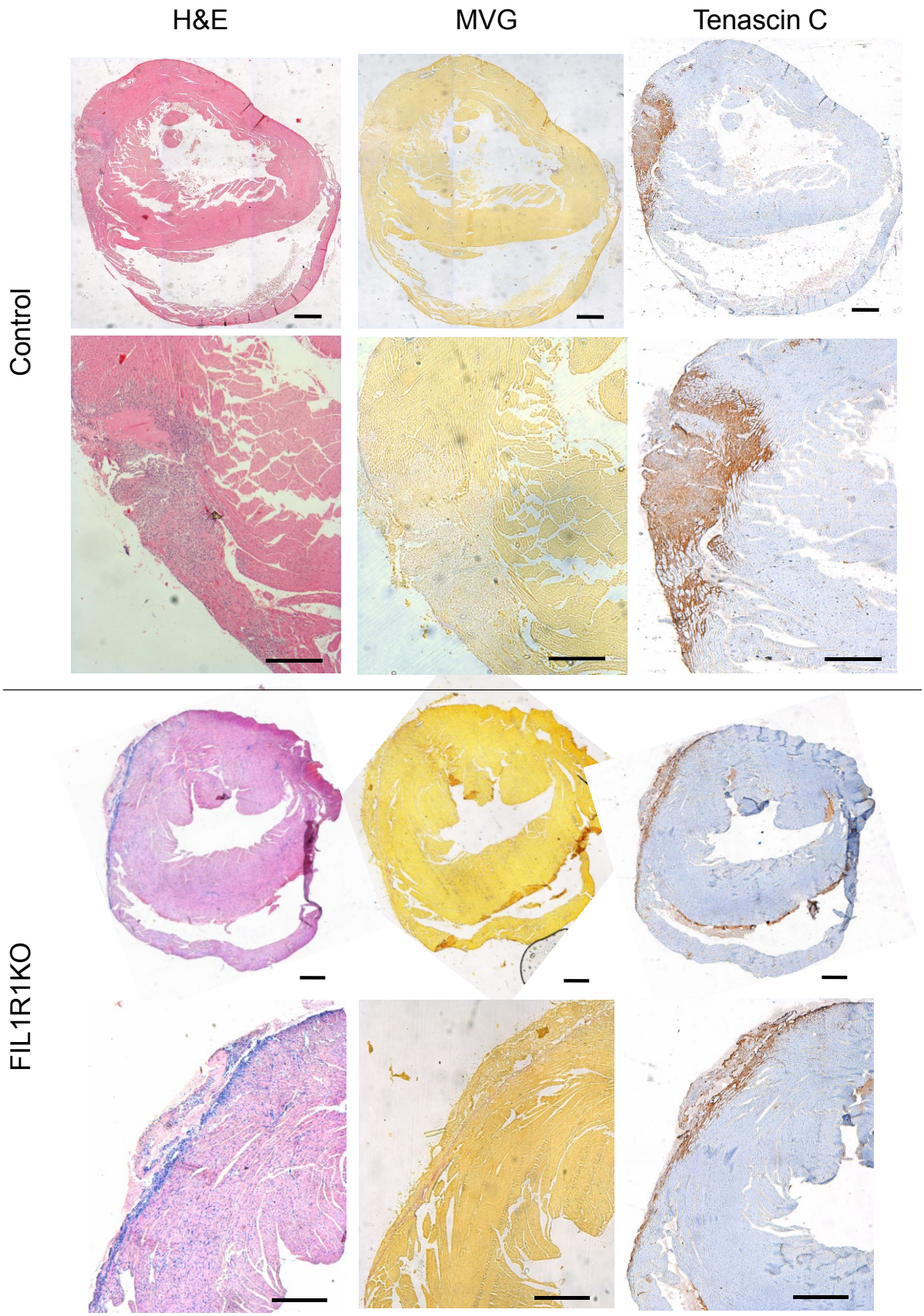
H&E
MVG
Tenascin C
Control
FIL1R1KO

Figure 6. Effect of fibroblast specific IL-R1 deletion on histological markers of cardiac remodelling 5 days post-MI. Representative photomicrographs of adjacent histological sections from Control and F1L1RKO (fibroblast-specific interleukin-1 receptor 1 knock out) hearts. *Left panels:* H&E staining showing inflammatory infiltrates and interstitial cells in the infarct zone. *Middle panels:* Miller's elastic van Gieson (MVG) staining showing elastin (blue) and collagen (pink) staining; muscle tissue is stained yellow. *Right panels:* Tenascin C staining (brown). Scale bars: 500μm.

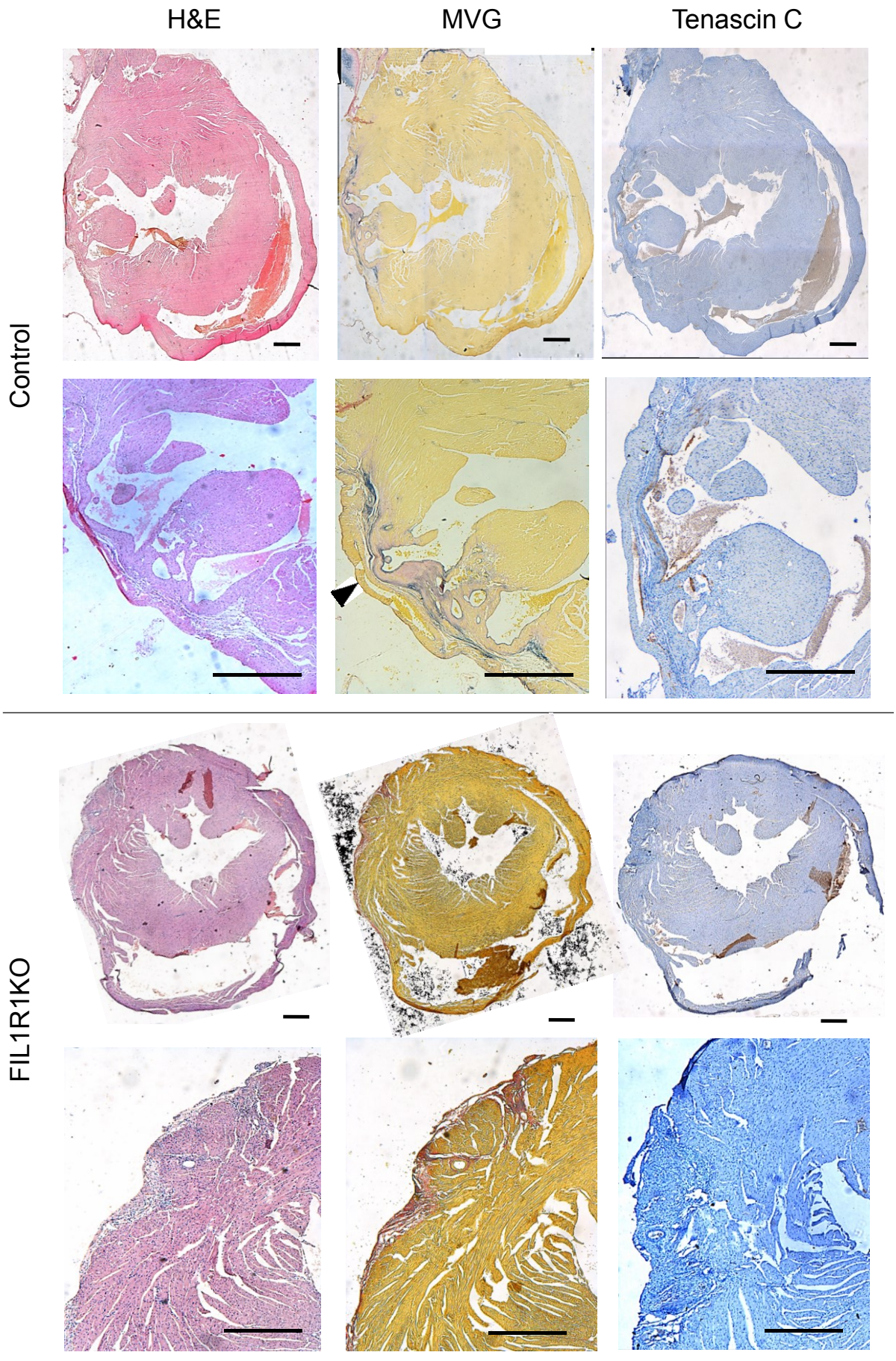
H&E
MVG
Tenascin C
Control
FIL1R1KO

Figure 7. Effect of fibroblast specific IL-R1 deletion on histological markers of cardiac remodelling 6 weeks post-MI. Representative photomicrographs of adjacent histological sections from Control and F1L1RKO (fibroblast-specific interleukin-1 receptor 1 knock out) hearts. *Left panels:* H&E staining showing inflammatory infiltrates and interstitial cells in the infarct zone. *Middle panels:* Miller's elastic van Gieson (MVG) staining showing elastin (blue) and collagen (pink) staining; muscle tissue is stained yellow. The area of ventricular thinning is indicated with an arrow head. *Right panels:* Tenascin C staining (brown). Scale bars: 500μm.